STATISTICAL AVERAGING IN ROTATIONALLY INELASTIC GAS–SURFACE SCATTERING: THE ROLE OF SURFACE ATOM MOTION

J.E. HURST Jr., G.D. KUBIAK and R.N. ZARE
Department of Chemistry, Stanford University, Stanford, California 94305, USA

Received 28 August 1982, in final form 23 September 1982

Within the framework of the one-dimensional cube model, the predicted appearance of rotational rainbows and trapping cutoffs in the final rotational state distribution in the limit of zero surface temperature is shown to depend strongly on statistical processes. In particular, inclusion of a distribution of initial surface cube velocities acts to broaden these features.

Recently, there have been many experimental investigations of rotationally inelastic gas–surface scattering using spectroscopic probes to extract both the final rotational state distributions [1–7] and the alignment [4] of a scattered diatomic gas. These results have stimulated renewed interest [8–10] in the simple classical one-dimensional "cube" models [11–13] of gas–surface scattering previously developed to explain the salient features of the observed angularly resolved flux distributions and, later, the final gas translational energy distributions. In this letter we demonstrate the effect of surface motion on the general features of the final gas rotational energy distribution, $P(E_\theta)$, predicted by a simpler stationary, infinite-mass surface cube model [8,9]: namely, the smearing of rotational rainbows and trapping cutoffs. This serves to illustrate the general behavior of such features when account is taken of the statistical averaging over the large number of degrees of freedom usually present in gas–surface collision systems.

First we summarize the general assumptions and predictions of the cube models in the limit of zero surface temperature with regard to the $P(E_\theta)$ function. In the "hard-cube" model the gas–surface interaction is assumed to be a one-dimensional, impulsive collision between the gas molecule, which is described by a shape, and the surface, which is described as a cube of finite mass. The interaction potential is given by.

$$U(Z,\theta) = 0, \quad Z > L(\theta), \qquad (1)$$
$$= \infty, \quad Z \leqslant L(\theta),$$

where Z is the distance of the molecular center of mass from the surface cube, $L(\theta)$ is the molecular shape function, and θ represents the set of angles necessary to describe the orientation of the molecule relative to the surface. We will restrict our discussion to diatomic gases which require only one such angle and therefore define θ as the angle between the internuclear axis and the surface normal. The diatomic is usually assumed to be elliptical in shape [13,14]. The center of this ellipse coincides with the midpoint of the nuclei and its major axis is parallel to the internuclear axis. The offset of the molecular center of mass from the midpoint of the nuclei present in a heteronuclear diatomic leads to an asymmetry in $L(\theta)$ [i.e. $L(\theta) \neq L(180 + \theta)$]. Hence, $L(\theta)$ depends on the size of the ellipsoid, characterized by the length of its major axis, a, its ellipticity, ϵ, defined as the ratio of the minor axis, b, to a, and the magnitude of the center-of-mass offset.

The requirement of infinite surface mass is relaxed by introducing as an additional parameter the mass ratio, $\mu = m/M$, where m is the effective surface mass and M the gas mass. This permits translational energy exchange between the gas and the surface. In addition, the possibility of a long-range attractive potential is included by introducing the well depth, E_w. The long-range nature of the attraction is treated by

0 009-2614/82/0000–0000/$ 02.75

assuming that only the gas particle is accelerated in the entrance channel and subsequently decelerated in the exit channel, i.e. the velocity of the gas–surface center of mass (c.m.) is altered in the attractive part of the potential. This is in contrast to gas-phase collisions where the c.m. velocity is constant throughout the collision.

More realistic models relax the hard or impulsive requirement leading to parameters which characterize the interaction potential between the gas and the cube. One such "soft-cube" potential considered here is

$$U(Z,\theta)/E_w = C_1[1 + A_1P_1(\cos\theta) + A_2P_2(\cos\theta)] \times \exp[n(1 - Z/R_0)] - (1 + C_1)(R_0/Z)^3, \quad (2)$$

where $C_1 = 3/(n-3)$ is a function of the repulsive parameter, n, and R_0 is the characteristic range parameter. The angular part of the potential is given by the constants A_1 and A_2 which are coefficients of the corresponding Legendre functions. In this particular potential the anisotropy is restricted to the repulsive part of the interaction, and the Z^{-3} dependence of the attractive portion of the potential is the result of averaging an inverse R^6 dependence over a continuum 3D solid. No attempt has been made to restrict the acceleration in the attractive region of the potential to the gas molecule as described above. This difference is minimized to some extent by the choice of a large value of μ used in the calculation.

The final rotational energy E_θ is calculated by smoothly varying θ in the range 0–π. Then $P(E_\theta)$ is formed according to

$$P(E_\theta) = \sum_i [P(\theta)|(d\theta/dE_\theta)|]_{\theta=\theta_i}, \quad (3)$$

where the sum is over all branches i that contribute population at E_θ. In eq. (3) $P(\theta)$ represents the weighting of initial polar angles. We take this as $\frac{1}{2}\sin\theta\,d\theta$, whereas other authors [12,13] appear to use a uniform weighting $d\theta/2\pi$. In the Monte Carlo calculations $P(E_\theta)$ is obtained directly by sampling θ in the range 0–π with a $\sin\theta$ weighting.

The theoretical $P(E_\theta)$ functions predicted by such models with no surface motion exhibit four general features depending on the form of the potential and the specific collision partners [‡].

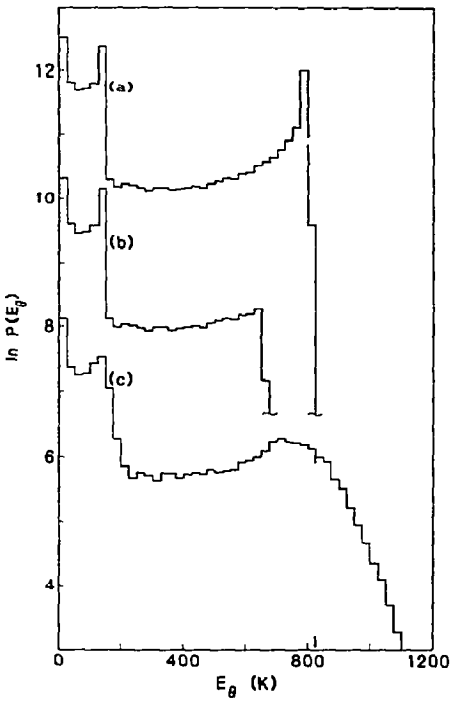

Fig. 1. Effect of surface temperature and well depth on the final rotational state distribution predicted by the hard-cube model. Shown are calculated ln $[P(E_\theta)]$ distributions obtained after 100000 trajectories using the moment of inertia and center of mass offset of $^{14}N^{16}O$ with a = 2.025 Å, ϵ = 0.939, μ = 14.052, for: (a) zero-temperature surface with no well and E_g = 2750 K; (b) zero-temperature surface with well depth E_w = 1500 K and E_g = 1250 K, and (c) same as (b) but with surface temperature of 800 K. For clarity (a)–(c) have been vertically displaced. The energy units are in K (1 K = 0.862 meV = 0.695 cm^{-1}).

(1) *Rainbow at $E_\theta = 0$.* A singularity occurs in $P(E_\theta)$ at $E_\theta = 0$ when there exists orientations of the gas molecule where $d\cos\theta/dE_\theta = \infty$ and $(\partial U/\partial\theta) = 0$ for all Z, i.e. the time-integrated torque on the molecule vanishes. Singularities arising because of local maxima

[‡] Note that the experimentally observed $P(E_\theta)$ necessarily include such effects as viewing factors, possible velocity- and wavelength-dependent detection efficiencies, etc., whereas the modeling takes none of these into account. The velocity correction could be important but to correct for it would require knowledge of the correlation between final translational and rotational energy states.

or minima in the classical excitation function, $E_\theta(\theta)$, are referred to as rainbows. For the simple ellipsoidal shape function used in the hard-cube model there are several angles where these conditions are met. Hence a rainbow is predicted as indicated in fig. 1. However there are many potentials where the criterion $d\cos\theta/dE_\theta = \infty$ is not met, such as the soft cube potential of eq. (2) when the coefficient of the P_1 term is much greater than that of the P_2 term. As illustrated in fig. 2b, $P(E_\theta)$ for this potential is relatively flat at low E_θ increasing gradually toward a rainbow of the type described below.

(2) *Rainbows at $E_\theta \neq 0$.* Additional rainbows occur when there exist orientations of the gas molecule where $(\partial U/\partial\theta) \neq 0$ and $d\cos\theta/dE_\theta = \infty$, i.e. there is a local maximum in the time-integrated torque on the molecule. For the ellipsoidal shape function with no offset c.m. this orientation leads to a rainbow in the $P(E_\theta)$ function when the collision is direct (has only one turning point in Z). The presence of an offset c.m. [i.e. an asymmetry in $L(\theta)$] results in a splitting of each rainbow into two rainbows whose energy spacing increases with increasing offset. For large transfer of translational energy into rotational excitation (caused by large c.m. offsets and/or large ellipticities), additional rainbows may appear even for direct collisions when the molecule is non-spherical. These rainbows are caused when one end of the molecule strikes the surface and then the other, such as in "cartwheeling" or "chattering" collisions [9], before the center of mass of the molecule has separated a sufficient distance from the surface cube. For the potentials used here *none* of the rainbows at $E_\theta \neq 0$ are the result of either cartwheeling or chattering. In the soft-cube potential described above, when $A_1 < 3A_2$, the P_1 term acts like an offset c.m. causing a doubling of the rainbow resulting from the P_2 term (see fig. 2). However, when $A_1 \geq 3A_2$, the low-energy component of the split rainbow moves past the rainbow at $E_\theta = 0$ and disappears. Finally, when $A_1 \gg A_2$ the rainbow at $E_\theta = 0$ is missing (see above) and only a single rainbow is predicted.

(3) *Trapping cutoff.* Hopping (indirect) trajectories may occur when a long-range attractive interaction is included in the model. In the context of the cube models these trajectories represent molecules which are usually assumed to equilibrate rapidly with the surface and hence appear in the trapping/desorption channel [‡]. In view of the simplistic way in which the cube models treat the surface it seems inappropriate to apply the model to hopping trajectories (especially on an infinite mass surface where only energy exchange between the various gas degrees of freedom is possible [8,9]). Because the angular distribution of this channel is broad relative to the direct channel, these particles are generally only a weak contribution to the specular signal and therefore are neglected. We are interested then in the way in which trapping affects $P(E_\theta)$ of the *direct* channel. Essentially, trapping removes the highest classically allowed final rotational energy states in the direct channel giving rise to a "trapping cutoff" (see fig. 1b). Since the highest classically allowed final rotational energy state occurs at the highest energy rainbow, trapping removes at least one rainbow from $P(E_\theta)$.

(4) *Alignment.* Because the potential functions used here are independent of the azimuthal angle, the

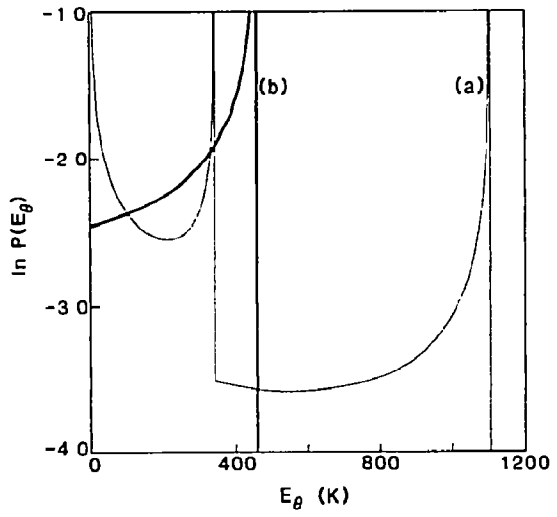

Fig 2. Effect of the parameters A_1 and A_2 on the final rotational distribution predicted by the cube model with the potential of eq (2) Shown are the calculated ln $[P(E_\theta)]$ distributions using the moment of inertia of $^{14}N^{16}O$. Parameters are n = 12, E_w = 1500 K, E_g = 1250 K, R_0 = 3 Å, μ = 14 052, for (a) $A_1 = A_2$ = 0 30, and (b) A_1 = 0 30, A_2 = 0.0.

‡ For theoretical discussions see, for example, ref [15], for experimental discussions demonstrating the lack of a scattering channel intermediate between direct and trapping desorption, see ref. [16]

final angular momentum lies in the plane of the surface except for any initial component of angular momentum along the surface normal which must be conserved in the collision. Since the incident gas in many of the available experimental results to date is a supersonic expansion, the incident angular momentum is very small (T_0 = 5–15 K) and does not result in appreciable depolarization of the final angular momentum.

It might be expected that the cube models would describe the scattering of molecules from surfaces having no appreciable corrugation [1–5]. Nevertheless, the experimentally observed $P(E_\theta)$ distributions differ in many respects from the simple picture presented above. The low-energy region does not exhibit the rainbow feature but instead can be characterized by a temperature. However, this trend of a decrease in the measured $P(E_\theta)$ with increasing E_θ in the low-E_θ region is consistent with that predicted by a potential featuring a rainbow at E_θ = 0 since, as shown in fig. 2b, the potential without a rainbow predicts an increasing $P(E_\theta)$. Experimental observation of rotational rainbows and alignment is available only for the case of NO on Ag(111) [3,4]. At high incident gas translational energy there does seem to be a feature at $E_\theta \neq 0$ which can be ascribed to a rotational rainbow, but the feature appears as a broad, ill-defined hump in the $P(E_\theta)$ function. Polarization experiments indicate that there is almost no polarization in the low-E_θ region of $P(E_\theta)$. However, the degree of polarization increases in the region of E_θ around the rainbow feature, followed by a very sharp transition to a second region of no polarization. No features attributable to multiple rainbows or trapping cutoffs have been observed

Better agreement between theory and experiment is obtained when the possibility of non-zero surface temperature is included in the cube models. For a cube model only the normal component of the relative velocity is important, its distribution is usually given by a relative-velocity-weighted gaussian at the surface temperature, T_s:

$$P_c(v_s) = A_c(1 - v_s/v_g)\exp(-mv_s^2/2k_bT_s), \qquad (4)$$

where $v_g = (2k_bE_g/m)^{1/2}$ is the incident gas velocity, and A_c is a normalization constant with $v_s/v_g \leqslant 1$. The result of a classical trajectory calculation averaged over gas geometry and surface motion is illustrated in fig. 1c. The $P(E_\theta)$ function predicted by the zero surface temperature model is modified in several aspects:

(1) The rainbow at E_θ = 0 is still a true classical singularity in the $P(E_\theta)$. In the cube approximation there is no correlation between surface velocity and those orientations of the gas where there is no net time-integrated torque. However, in many cases the decrease in $P(E_\theta)$ with E_θ is much less pronounced, indicating a broadening of the rainbow. Certainly a quantum mechanical treatment of the interaction would remove the rainbow at low E_θ [10,14,17,18].

(2) In contrast to the effect of surface motion on the rainbow at E_θ = 0, the other rainbow features are considerably broadened and are no longer actual classical singularities in the $P(E_\theta)$ function. The sensitivity of the rainbows is not surprising since there are no local maxima in the $E_\theta(\theta, v_s)$ function, increasing surface cube velocity leads to increasing final gas rotational energy. However, there is still a residual peaking in $P(E_\theta)$ near the energy where the zero surface temperature rainbow occurred because of the form of eq. (4) and surface temperatures used.

(3) The trapping cutoff is also considerably broadened. In an impulsive collision model this results from the linear correlation between the incident relative velocity of the collision and the final angular momentum of the gas. This is a strong effect since the distribution of surface velocity directly modify the relative velocity of the collision, making possible final rotational energies greater than the incident translational energy of the gas.

(4) There is no change in the polarization from that predicted by the zero surface temperature model.

Although the inclusion of surface motion by no means corrects all the qualitative differences between the simple one-dimensional models for gas–surface interactions and the observed final rotational state distributions, it does considerably better than both infinite surface mass and zero surface temperature models. Moreover, it provides insight into the important role of statistical averaging in such modeling. The main qualitative discrepancy still remaining is the strict polarization required by the assumption of an azimuthally independent potential. The simplest way to remove this restriction is to include surface corrugation, either as a hard corrugated wall in the impulsive limit or by modulating the potential of eq. (2)

over the unit cell. Corrugation will lead to additional smearing of most of the simple features manifest in the $P(E_\theta)$ function since three new coordinates must be added to the calculation.

As pointed out above, a complete quantum-mechanical treatment of the scattering problem would smooth out the singularities in $P(E_\theta)$ predicted by classical mechanics. Our preliminary calculations using a closed-form approximate solution [14] to the quantum-mechanical scattering of an ellipsoid from a wall indicate that the rainbow at $E_\theta = 0$ is much less pronounced and the rainbows at higher E_o are even more attenuated and broadened. A coupled-channel calculation has recently been performed by Barker et al. [10] also indicating these results.

In summary, we have demonstrated how the inclusion of surface motion within the framework of the cube models leads to a broadening of the rotational rainbow at $E_\theta = 0$, the higher-energy rainbows, and the trapping cutoff. These effects are expected to be a general result whenever the rotational degree of freedom of the gas is coupled to another degree of freedom which must be treated statistically. Certainly additional statistical processes are operative in the observed experimental results since the measured rotational alignment indicates significant depolarization in the low-E_θ region of the $P(E_\theta)$ function. Quantum-mechanical modeling of the interaction also leads to broad features in the final $P(E_\theta)$ function. In view of the sensitivity of the calculated $P(E_\theta)$ function for direct scattering to statistical averaging perhaps it is not surprising that (a) the experimentally observed $P(E_\theta)$ can be characterized by a temperature in the low-E_θ region, and (b) the rainbows at $E_\theta \neq 0$ and the trapping cutoff are considerably smeared. We stress that the usefulness of such simple models lies not in their ability to reproduce accurately the final distributions in the various degrees of freedom of the scattered gas molecule, but rather, in their ability to predict trends in coarser parameters such as the moment parameters characterizing the angular flux distributions, the mean exit translational energy, and the mean exit rotational energy.

We thank D.J. Auerbach for useful discussions and a critical reading of this manuscript. This work was supported by the Army Research Office under DAAG-29-80-K-0035 and the Office of Naval Research under N00014-78-C-0403. RNZ gratefully acknowledges support through the Shell Distinguished Chairs Program, funded by the Shell Companies Foundation, Inc.

References

[1] F. Frenkel, J. Häger, W. Krieger, H. Walther, C.T. Campbell, G. Ertl, H. Kuipers and J. Segner, Phys. Rev. Letters 46 (1981) 152.
F. Frenkel, J. Häger, W. Krieger, H. Walther, G. Ertl, J. Segner and W. Vielhaber, Chem. Phys. Letters 90 (1982) 225
[2] G.M. McClelland, G.D. Kubiak, H.G. Rennagel and R.N. Zare, Phys. Rev. Letters 46 (1981) 831,
G.D. Kubiak, J.E. Hurst Jr., H.G. Rennagel, G.M. McClelland and R.N. Zare, to be published
[3] A.W. Kleyn, A.C. Luntz and D.J. Auerbach, Phys. Rev. Letters 47 (1981) 1169, J. Chem. Phys. 76 (1982) 737
[4] A.W. Kleyn, A.C. Luntz, and D.J. Auerbach, Phys. Rev. B25 (1982) 4273
[5] M. Asscher, W.L. Guthrie, T.-H. Lin and G.A. Somorjai, Phys. Rev. Letters 49 (1982) 76
[6] J.W. Hepburn, F.J. Northrup, G.L. Ogram, J.C. Polanyi, and J.M. Williamson, Chem. Phys. Letters 85 (1982) 127,
D. Littinger, K. Honma, M. Keil and J.C. Polanyi, Chem. Phys. Letters 87 (1981) 413
[7] R.R. Cavanagh and D.S. King, Phys. Rev. Letters 47 (1981) 1829.
[8] J.M. Bowman and S.C. Park, J. Chem. Phys. 76 (1982) 1168, to be published
[9] J.C. Polanyi and R.J. Wolf, Ber. Bunsenges. Physik. Chem. 86 (1982) 356
[10] J.A. Barker, A.W. Kleyn and D.J. Auerbach, to be published
[11] R.M. Logan and R.E. Stickney, J. Chem. Phys. 44 (1966) 195,
R.M. Logan and J.C. Keck, J. Chem. Phys. 49 (1968) 860
[12] J.D. Doll, J. Chem. Phys. 59 (1973) 1038
[13] W.L. Nichols and J.H. Weare, J. Chem. Phys. 62 (1975) 2754, 63 (1975) 279, 66 (1977) 1075
[14] V. Garibaldi, A.C. Levi, R. Spadacini and G.E. Tommei, Surface Sci. 55 (1976) 40.
[15] F.O. Goodmann, in Rarefied gas dynamics, Vol. 2, ed. J.H. de Leeuw (Academic Press, New York, 1966) p. 366,
R.A. Oman, J. Chem. Phys. 48 (1968) 3919
[16] J.E. Hurst Jr., C.A. Becker, J.P. Cowin, K.C. Janda, L. Wharton and D.J. Auerbach, Phys. Rev. Letters 43 (1979) 1175
[17] P.E. Fitz, A.O. Bawagan, L.H. Beard, D.J. Kouri and R.B. Gerber, Chem. Phys. Letters 80 (1981) 537
[18] R. Schinke, J. Chem. Phys. 76 (1982) 2352